Differential Metabolic Sensitivity of Insulin-like-response- and mTORC1-Dependent Overgrowth in *Drosophila* Fat Cells

Maelle Devilliers[1], Damien Garrido[1,‡], Mickael Poidevin[1], Thomas Rubin[1,§], Arnaud Le Rouzic[2], and Jacques Montagne[1,*]

[1] Institute for Integrative Biology of the Cell (I2BC), CNRS, Université Paris-Sud, CEA, F-91190, Gif-sur-Yvette, France

[2] Laboratoire Evolution, Génomes, Comportement et Ecologie, CNRS, Université Paris-Sud, UMR 9191, F-91190, Gif-sur-Yvette, France

* Correspondence: Jacques.MONTAGNE@i2bc.paris-saclay.fr

‡ Present address: IRIC, Université de Montréal, Montréal, Québec H3T 1J4, Canada

§ Present address: Institut Curie, CNRS UMR 3215 / INSERM U-934, F-75248 Paris Cedex 5

Running title: Metabolism and mTOR network

Key words: Lipogenesis, Glycolysis, cell-autonomous effect, homeostasis

ABSTRACT

The glycolytic/lipogenic axis promotes the synthesis of energetic molecules and building blocks necessary to support cell growth, although the absolute requirement of this metabolic axis must be deeply investigated. Here, we used *Drosophila* genetics and focus on the mTOR signaling network that controls cell growth and homeostasis. mTOR is present in two distinct complexes, mTORC1 and mTORC2. The former directly responds to amino acids and energetic levels, whereas the latter is required to sustain the signaling response downstream of insulin-like-peptide (Ilp) stimulation. Either signaling branch can be independently modulated in most *Drosophila* tissues. We confirm this independency in the fat tissue. We show that ubiquitous over-activation of mTORC1 or Ilp signaling affects carbohydrate and lipid metabolism, supporting the use of *Drosophila* as a powerful model to study the link between growth and metabolism. We show that cell-autonomous restriction of glycolysis or lipogenesis in fat cells impedes overgrowth dependent on Ilp- but not mTORC1-signaling. Additionally, ubiquitous deficiency of lipogenesis (*FASN* mutants) results in a drop in mTORC1 but not Ilp signaling, whereas, at the cell-autonomous level, lipogenesis deficiency affects none of these signals in fat cells. These findings thus, reveal differential metabolic sensitivity of mTORC1- and Ilp-dependent overgrowth. Furthermore, they suggest that local metabolic defects may elicit compensatory pathways between neighboring cells, whereas enzyme knockdown in the whole organism results in animal death. Importantly, our study weakens the use of single inhibitors to fight mTOR-related diseases and strengthens the use of drug combination and selective tissue-targeting.

INTRODUCTION

Growth of a multicellular organism is coordinated by signaling pathways that adjust intracellular processes to environmental changes. These signaling pathways include the mTOR (mechanistic Target Of Rapamycin) regulatory network that integrates the growth factor response as well as the nutritional and energetic status (LAPLANTE AND SABATINI 2012; HOWELL *et al.* 2013; LAMMING AND SABATINI 2013; SHIMOBAYASHI AND HALL 2014; CARON *et al.* 2015; SAXTON AND SABATINI 2017; MOSSMANN *et al.* 2018). Activation of this network promotes basal cellular functions, thereby providing building blocks to sustain cellular growth. However, despite a plethora of studies on the mTORC signaling network, the requirement of basal metabolism—glycolytic/lipogenic axis— for cell growth has not been systematically investigated. The *Drosophila* model provides a powerful genetic system to address these issues (UGUR *et al.* 2016), since both the intermediates of this signaling network and the basal metabolic pathways are conserved in the fruit fly (MONTAGNE *et al.* 2001; HAY AND SONENBERG 2004; PADMANABHA AND BAKER 2014; ANTIKAINEN *et al.* 2017; WANGLER *et al.* 2017; LEHMANN 2018).

The mTOR protein kinase is present in two distinct complexes, mTORC1 and mTORC2 that comprise raptor and rictor, respectively (KIM *et al.* 2002; SARBASSOV *et al.* 2005). Regulation of mTORC1 activity by ATP and amino acids depends on a multi-step process that results in the recruitment of an mTORC1 homodimer at the lysosomal membrane in the vicinity of the small GTPase Rheb (Ras homologue enriched in brain) (GOBERDHAN *et al.* 2009; MA AND BLENIS 2009; DIBBLE AND MANNING 2013; GROENEWOUD AND ZWARTKRUIS 2013; MONTAGNE 2016). Rheb stimulates mTORC1 activity (YANG *et al.* 2017), which in turn regulates several downstream targets. S6Kinase1 (S6K1) is one such kinase, sequentially activated through the phosphorylation of its T389 and T229 residues by mTORC1 and by PDK1 (Phosphoinositide-dependent protein kinase 1),

70 respectively (MONTAGNE AND THOMAS 2004; MAGNUSON *et al.* 2012). Further, Rheb
71 activation of mTORC1 is repressed by the tumor suppressor TSC (Tuberous sclerosis
72 complex) that comprises subunits TSC1 and TSC2 (RADIMERSKI *et al.* 2002a; GARAMI *et*
73 *al.* 2003; INOKI *et al.* 2003a; DIBBLE *et al.* 2012). The integrity of mTORC2 is required to
74 sustain the downstream insulin-signaling response (SARBASSOV *et al.* 2005). Binding of
75 insulin or related peptides (Ilps) to their cognate receptors results in recruitment of class
76 I PI3K (Phosphoinositide 3-kinase) to the membrane. PI3K phosphorylates inositol lipids
77 producing phosphatidylinositol-3,4,5-triphosphate (PIP3) (ENGELMAN *et al.* 2006;
78 HAEUSLER *et al.* 2018), while the tumor suppressor PTEN acts as a lipid phosphatase to
79 counteract this process (CULLY *et al.* 2006; GOBERDHAN *et al.* 2009). PIP3 constitutes a
80 membrane docking site for the protein kinase Akt whose activity requires the
81 subsequent phosphorylation of its S473 and T308 residues by mTORC2 and PDK1,
82 respectively (LIEN *et al.* 2017).

83 Constitutive activation of mTORC1 in MEFs (Mouse embryonic fibroblasts) has been
84 shown to stimulate a metabolic network, including glycolysis, the pentose phosphate
85 pathway and the biosynthesis of fatty acid (FA) and cholesterol (DUVEL *et al.* 2010).
86 Most of the genes encoding glycolytic enzymes are over-expressed in these cells as are
87 those encoding LDH (lactate dehydrogenase) and Pdk1 (Pyruvate dehydrogenase
88 kinase 1; an inhibitor of mitochondrial pyruvate processing). This suggests that
89 mTORC1-activated MEFs potentiate anaerobic glycolysis and repress the tricarboxylic
90 acid (TCA) cycle. Conversely, adipose-specific knockout of raptor to impede mTORC1
91 formation, results in enhanced uncoupling of mitochondrial activity (POLAK *et al.* 2008).
92 The increased lipogenesis observed in mTORC1 stimulated cells depends on a
93 downstream transcriptional regulatory axis involving the cofactor Lipin 1 along with a
94 SREBP (Sterol responsive element binding-protein) family member, which activates

genes encoding lipogenic enzymes (DUVEL *et al.* 2010; PETERSON *et al.* 2011). Congruently, another study revealed that TSC2 mutant cells become addicted to glucose as a result of mTORC1 hyper-activity (INOKI *et al.* 2003b). In addition, inhibition of mTORC1 activity revealed that these TSC2 mutant cells become also dependent on glutamine catabolism (CHOO *et al.* 2010); mTORC1 potentiates this catabolism to feed TCA anaplerosis, through 1) a S6K/eIF4B/Myc axis that increases glutaminase protein levels (CSIBI *et al.* 2014) and 2) the repression of SIRT4, a mitochondrial sirtuin that inhibits glutamine dehydrogenase (CSIBI *et al.* 2013). Besides mTORC1 mediated regulation, Ilp-signaling also impinges on basal metabolism. Intracellular activation of Akt increases ATP levels (HAHN-WINDGASSEN *et al.* 2005; ROBEY AND HAY 2009) through the stimulation of GLUT4-mediated glucose uptake (JALDIN-FINCATI *et al.* 2017) and the enhancement of the expression and activity of glycolytic enzymes (GOTTLOB *et al.* 2001; HOUDDANE *et al.* 2017). Akt also dampens glucose production by suppressing PEPCK (gluconeogenesis), glucose-6-phosphatase (glycogenolyse) and the glycogen synthesis repressor GSK3 (NAKAE *et al.* 2001; MCMANUS *et al.* 2005). However, in contrast to mTORC1, Akt also promotes mitochondrial metabolism and oxidative phosphorylations (GOTTLOB *et al.* 2001; MAJEWSKI *et al.* 2004). Conversely, hepatic knockout of the mTORC2 specific-subunit rictor results in constitutive gluconeogenesis and impaired glycolysis and lipogenesis (HAGIWARA *et al.* 2012; YUAN *et al.* 2012). Taken together, these studies strongly emphasize the role of mTOR in metabolic-related diseases and in adjusting metabolism to the nutritional and energetic status (MOSSMANN *et al.* 2018).

In the present study, we investigated the requirement of the glycolytic/lipogenic axis for the cellular growth induced by hyper-activation of mTORC1 signaling and Ilp response in *Drosophila*. As previously demonstrated, mTORC1 and Ilp signaling reside on independent branches in most *Drosophila* tissues (RADIMERSKI *et al.* 2002a; RADIMERSKI

120 *et al.* 2002b; DONG AND PAN 2004; MONTAGNE *et al.* 2010; PALLARES-CARTES *et al.* 2012).
121 Here, we confirmed this independency in the *Drosophila* fat body (FB), the organ that
122 fulfils hepatic and adipose functions to control body homeostasis (PADMANABHA AND
123 BAKER 2014; ANTIKAINEN *et al.* 2017; LEHMANN 2018). We show that ubiquitous over-
124 activation of mTOR or Ilp signaling provokes an apparent enhancement of metabolite
125 consumption. Furthermore, our study reveals that metabolic restriction at the organismal
126 level has dramatic consequences on animal survival, but minor effect at the cell-
127 autonomous level, suggesting that within an organism, alternative pathways may
128 operate to compensate local metabolic defects. Nonetheless, at the cell-autonomous
129 level, metabolic restriction can partially restrain overgrowth dependent on hyper-
130 activation of Ilp- but not mTORC1-signaling, indicating that the potential compensatory
131 metabolic pathways do not fully operate in the context of Ilp-signaling stimulation.

132

133 **MATERIAL & METHODS**

134 **Genetics and fly handling**

135 Fly strains: *P[w[+mC]=tubP-GAL80]LL10,P[ry[+t7.2]=neoFRT]40A*, *daughterless(da)-*
136 *gal4*, *tub-gal80^{ts}*, *UAS-Dcr-2* (Bloomington Stock Center); *FASN$^{1-2}$* (GARRIDO *et al.*
137 2015); *mTOR$^{\Delta P}$* (ZHANG *et al.* 2000); *mTOR^{2L1}* and *PTEN* (OLDHAM *et al.* 2000);
138 *EP(UAS)-Rheb* (STOCKER *et al.* 2003);); inducible interfering RNA (*UAS-RNAi*) lines to
139 *PTEN* (NIG 5671R-2), *FASN1* (VDRC 29349), *PFK1* (VDRC 3017), *PK* (VDRC 49533)
140 *PDH* (VDRC 40410), *LDH* (VDRC 31192) (DIETZL *et al.* 2007). The *Minute* stock used
141 was previously referred to as *FRT40/P(arm-LacZ w^{+})* (BOHNI *et al.* 1999) but exhibit
142 both developmental delay and short and slender bristles, typically reported as *Minute*
143 phenotype (MORATA AND RIPOLL 1975). To generate MARCM clones in the *Minute*

144 background, these flies were recombined with the *P[w[+mC]=tubP-*
145 *GAL80]LL10,P[ry[+t7.2]=neoFRT]40A* chromosome.

146 The standard media used in this study contained agar (1g), polenta (6g) and yeast (4g)
147 for 100ml. Lipid- (beySD) and sugar-complemented media were prepared as previously
148 described (GARRIDO *et al.* 2015).

149 To select *FASN*$^{1-2}$ mutant larvae, we used a GFP-labelled CyO balancer chromosome.
150 Flies were let to lay eggs on grape juice plates for less than 24 hrs. Then, some beySD
151 media was put in the middle of the plates; larvae that do not express GFP were
152 collected the next day and transferred to fresh tubes. Prepupae were collected once a
153 day to evaluate developmental delay and to measure body weight.

154

155 **Molecular biology and Biochemistry**

156 To test RNAi-knockdown efficacy to the glycolytic enzymes (Figure S2), *UAS-Dcr-2;da-*
157 *gal4,tub-gal80*^{ts} virgin females were mated with UAS-RNAi males. Flies were let to lay
158 eggs overnight and tubes were kept at 19°C for two days. Tubes were then transferred
159 at 29°C and two days later, larvae of roughly the same size were collected. Reverse
160 transcription and quantitative PCR were performed as previously described (PARVY *et*
161 *al.* 2012).

162 Protein extracts for western-blotting were prepared as previously described (MONTAGNE
163 *et al.* 2010). Antibody used in for western-blotting have been previously described
164 (MONTAGNE *et al.* 2010) or commercially provided for Akt (Cell signaling 4054).

165 For metabolic measurements, parental flies were let to lay eggs in tubes for less than 24
166 hrs at 25°C. Tubes were then transferred at 29°C to strengthen the gal4/UAS effect,
167 and using a *UAS-Dcr-2* to strengthen the RNAi effect. Larvae were either maintained in

168 the same tubes or selected prior to L2/L3 transition and transferred on 20%-SSD.
169 Collection of prepupae and metabolic measurements were performed as previously
170 described (GARRIDO *et al.* 2015).

171

172 **Clonal analysis**

173 All the clones were generated using the MARCM strategy (LEE AND LUO 2001). Parental
174 flies were let to lay eggs at 25°C for seven hrs. Tubes were then heat shocked for 65
175 minutes in a water bath at 38°C so that recombination happens while FB precursor cells
176 are in dividing process. FB from feeding larvae at the end of the L3 stage where
177 dissected, fixed, membranes were labelled with phalloidin and nuclei with DAPI, and FB
178 were mounted as previously described (GARRIDO *et al.* 2015). Image acquisitions were
179 obtained using a Leica SP8 confocal laser-scanning microscope. For immuno staining
180 the phospho-S6 antibody has been previously described (ROMERO-POZUELO *et al.*
181 2017) and the phospho-Akt commercially provided (Cell signaling 4054). The cell size
182 calculation have been performed as previously described (GARRIDO *et al.* 2015) and
183 correspond to a set of experiments that spanned a two-year period. It represent too
184 many replicates, so that it was not possible to make them at the same time. Therefore,
185 for the graphs of cell size measurement (Figure 1M, 5M and 7M), values are reused
186 when they correspond to the same genotype and conditions. This allows a direct
187 comparison between the experiments.

188

189 **Statistical analysis**

190 Statistical analyses were performed with R version 3.4.4, scripts are available on
191 request. Significance for the statistical tests was coded in the following way based on

the p-values: ***: 0 < p < 0.001; **: 0.001 < p < 0.01; *: 0.01 < p < 0.05. P-values were corrected for multiple testing by a Holm-Bonferroni method (HOLM 1079). Clone sizes were analyzed with a mixed-effect linear model on the logarithm of cell area, considering the treatment (Genotype and Sucrose conditions) as a fixed effect and Series/Larva as random effects (Figures 1, 5, and 7, Table S1). The reported effects (and the corresponding P-values) were obtained from the difference between the (log) area of marked clonal cells and that of control surrounding cells from the same treatment, by setting the appropriate contrast with the "multcomp" package (HOTHORN *et al.* 2008), according to the pattern: EA,B = log(MA) – log(WA) – [log(MB) – log(WB)], where EA,B is the difference between treatments (genotype and sucrose levels) A and B, MA and MB standing for the area of marked cells, and WA, WB for the area of control cells in those treatments. This is equivalent to testing whether marked/control cell area ratios differ between treatments. PS6+ clone frequencies were treated as binomial measurements in a mixed-effect generalized linear model "lme4" package (BATES *et al.* 2015), featuring Genotype as a fixed effect, and Series/Larva as random effects. Both datasets of pupal weights were analyzed independently with linear models including Sex, Genotype, and Sucrose level effects and all their interaction terms (Figure 3A-B and Table S3 for PTEN knockdown and Rheb overexpression; Figure 6B and Table S4 for *FASN*$^{1-2}$ mutants). TAG, Protein, Glycogen, and Threalose concentrations were also analyzed with linear models involving Genotype, Sucrose level, and their interactions as fixed effects (Figure 3 and Table S3).

Data and reagent availability statement

Fly stocks are available upon request. Supplementary materials include Figures S1-S2, Tables S1-S4 and supdata/script files available on the GSA figshare portal.

RESULTS

mTORC1 and Ilp signaling independency in the fat body

Activating either the mTORC1 or the Ilp signaling branch can be performed by overexpressing Rheb or depleting PTEN, respectively. To investigate this independency in the FB, we generated somatic clones either over-expressing Rheb (*Rheb*$^{+}$) (STOCKER *et al.* 2003) or homozygote for a *PTEN* mutation (*PTEN*$^{-/-}$) (OLDHAM *et al.* 2000). The precursors of FB cells divide in the embryo; during larval life, the differentiated cells do not divide but endoreplicate their DNA content to reach a giant size (EDGAR AND ORR-WEAVER 2001). Therefore, to precisely evaluate the effect on cell growth, somatic recombination events were induced during embryogenesis at the stage of proliferation of the FB cell precursors and the resulting MARCM clones were analyzed in the FB of late feeding L3 larvae, prior to the wandering stage that precedes metamorphosis entry. Both *PTEN*$^{-/-}$ and *Rheb*$^{+}$ clonal cells were bigger than the surrounding control cells and this cell size effect was dramatically increased in *PTEN*$^{-/-}$;*Rheb*$^{+}$ combined clones (Figure 1A-D and 1M). We next analyzed this growth increase in the context of the previously described *mTOR*^{2L1} and *mTOR*$^{\Delta P}$ mutations. However, we could not find mutant clones in the FB. Consistent with previous studies reporting that mTOR is critically required for cell growth of endoreplicative tissues (OLDHAM *et al.* 2000; ZHANG *et al.* 2000), we reasoned that these clonal cells were likely eliminated by cell competition (MORATA AND RIPOLL 1975). Thus, we generated somatic clones in a *Minute* background to slow down the growth of the surrounding control cells. In these conditions, *mTOR* mutant clones could indeed be recovered. Both *mTOR*^{2L1} and *mTOR*$^{\Delta P}$ mutant cells exhibited a dramatic size reduction (Figure 1G and 1J) and this phenotype was dominant in *Rheb*$^{+}$ combined clonal cells (compare Figure 1E to 1H and

1K). In contrast, *mTOR*$^{\Delta P}$ but not *mTOR*^{2L1} exhibited a clear dominant phenotype over the *PTEN*$^{-/-}$ mutation; the size of *mTOR*$^{\Delta P}$,*PTEN*$^{-/-}$ clonal cells was dramatically reduced, whereas *mTOR*^{2L1},*PTEN*$^{-/-}$ clonal cells were giant (compare Figure 1F to 1I and 1L). These findings indicate that the *mTOR*^{2L1} mutation affects mTORC1 but not Ilp signaling, whereas *mTOR*$^{\Delta P}$ affects both signaling branches.

Next, we used phospho-specific antibodies in immunostaining assays to analyze the phosphorylation of Akt (P-Akt) and of the dS6K target, ribosomal protein rpS6 (P-S6). In *PTEN*$^{-/-}$ clonal cells, we observed an increase in the P-Akt intracellular signal (Figure 2A). Importantly the P-Akt intracellular signal was absent in *mTOR*$^{\Delta P}$ cells (Figure 2B) but not affected in *mTOR*^{2L1} cells (Figure 2C). Staining with the rpS6 phospho-specific antibody revealed a patchy signal, with only a subset of cells expressing the P-S6 signal in the FB (Figure 2E-J), a pattern previously described in the wing imaginal disc (ROMERO-POZUELO *et al.* 2017). Therefore, to evaluate mTORC1 activity, we measured the ratio of P-S6 positive cells among the population of GFP^{+} clonal cells. For control clones, only labeled by GFP, about half of them were P-S6 positive (Figure 2E and 2K), whereas most of the *mTOR*^{2L1} and *mTOR*$^{\Delta P}$ clones were P-S6 negative (Figure 2F, 2G and 2K). Importantly, almost all the *Rheb*$^{+}$ cells were P-S6 positive (Figure 2H and 2K), whereas the ratio of P-S6 positive cells was slightly but not significantly increased in the *PTEN*$^{-/-}$ cell population (Figure 2I and 2K). Taken together, these findings confirm that mTORC1 and Ilp signaling operate independently in FB cells and reveal that the *mTOR*^{2L1} mutation affects only mTORC1, whereas the *mTOR*$^{\Delta P}$ mutation affects both signaling branches.

Activating mTORC1 or Ilp signaling impacts basal metabolism

A number of studies support the notion that the mTOR signaling network controls metabolism to sustain cellular growth. To evaluate how mTORC1 and Ilp affect basal metabolism in *Drosophila*, we analyzed various metabolites in whole animals that express the ubiquitous *da-gal4* driver to direct Rheb overexpression (*Rheb*$^{++}$) or PTEN knockdown by RNA interference (*PTEN-RNAi*). Larvae were fed either a standard or a 20%-sucrose supplemented diet (20%-SSD) and 0-5h prepupae were collected, as this is a convenient phase to stage the animals after the feeding period. When fed a standard diet, a high rate of lethality was observed for *Rheb*$^{++}$ and *PTEN-RNAi* larvae, although a sufficient number of prepupae could be collected for metabolic analysis. In contrast, none of the *Rheb*$^{++}$ and *PTEN-RNAi* larvae reached the prepupal stage when fed a 20%-SSD. Nonetheless, when *Rheb*$^{++}$ and *PTEN-RNAi* larvae were fed a standard diet during early larval life and transferred onto a 20%-SSD at the L2/L3 molting transition, we could recover a few prepupae for metabolic measurements. For both males and females fed a standard diet, the body weight of *Rheb*$^{++}$ and *PTEN-RNAi* prepupae was roughly similar to that of controls (Figure 3A and 3B). Conversely, providing a 20%-SSD resulted in a drop of the prepupal weight of control animals that was significantly compensated in *Rheb*$^{++}$ and *PTEN-RNAi* prepupae (Figure 3A and 3B).

Next, we measured the total amounts of protein, triacylglycerol (TAG), glycogen and trehalose—the most abundant circulating sugar in *Drosophila*. Although variations in protein levels were observed, none of them were statistically significant (Figure 3C). TAG levels in control prepupae were not affected by sucrose supplementation and did not vary in *PTEN-RNAi*, but were significantly decreased in *Rheb*$^{++}$ animals (Figure 3D). Feeding larvae a 20%-SSD since the L2/L3 molting transition resulted in a marked in increase in glycogen and trehalose levels in control prepupae (Figure 3E-F). In *Rheb*$^{++}$

and, in lower extent, in *PTEN-RNAi* prepupae, glycogen levels were significantly lower than those measured in controls (Figure 3E). Finally, trehalose levels were strongly decreased in both *Rheb*$^{++}$ and *PTEN-RNAi* prepupae fed either a standard or a 20%-SSD as compared to the control (Figure 3F). Taken together, these findings suggest that a ubiquitous increased activity of either mTORC1 or Ilp signaling provokes an apparent increase in metabolite consumption. This metabolic rate is correlated with a relative increase in body weight for larvae fed a 20%-SSD, but not for those fed a standard diet. We previously observed that increasing dietary sucrose induced a reduction in food intake (GARRIDO *et al.* 2015) that may account for the body weight reduction of control animals. Potentially, food intake could be less affected in *Rheb*$^{++}$ and *PTEN-RNAi* animals, thereby leading to a compensatory effect on body weight. Measuring food intake in *Rheb*$^{++}$ or *PTEN-RNAi* larvae was not applicable since most of them die during larval stage and thus, terminate feeding earlier. In sum, our data indicates that basal metabolism is altered in the few *Rheb*$^{++}$ or *PTEN-RNAi* larvae that survive and further suggests that in most cases stronger metabolic disruption happened, resulting in lethal homeostatic defects.

Knocking-down glycolysis at the whole body level

Since manipulating mTOR resulted in a decrease in the levels of TAG and glycogen stores and of circulating trehalose (Figure 3), we asked whether the basal energetic metabolism affected mTORC1- and/or Ilp-signaling. First, we ubiquitously expressed interfering RNA against phosphofructokinase1 (*PFK1-RNAi*), pyruvate kinase (*PK-RNAi*) pyruvate dehydrogenase (*PDH-RNAi*) and lactate dehydrogenase (*LDH-RNAi*). PFK1 catalyzes the third glycolytic reaction to form fructose 1,6-bisphophate; PK catalyzes the final glycolytic reaction to form pyruvate; PDH directs the mitochondrial

316 fate of pyruvate, whereas LDH directs its anaerobic fate (Figure 4A). When directed with
317 the ubiquitous *da-gal4* driver, *PK-RNAi* provoked early larval lethality, *PFK1-RNAi* and
318 *PDH-RNAi* provoked larval lethality at L2 or L3 stages, whereas *LDH-RNAi* induced a
319 semi-lethal phenotype at larval or pupal stages (Figure 4B).

320 Second, we monitored the phosphorylation of the *Drosophila* S6Kinase (dS6K) and Akt
321 as read-out of the activity of mTORC1- and Ilp-signaling respectively. To circumvent the
322 early lethality, the *da-gal4* driver was combined with a ubiquitous thermo-sensitive form
323 of the Gal4 inhibitor, Gal80^{ts} (*tub-gal80^{ts}*) that blocks Gal4 activity at 21°C but not at
324 29°C, thereby allowing RNAi expression after temperature shift. Each RNAi was
325 ubiquitously induced at early L1 stage and protein extracts were prepared two days later
326 using late L2 larvae. At this stage the larvae were still viable, although those expressing
327 PK-RNAi did not undergo L2/L3 transition and eventually died (Figure 4B). Western-
328 blotting using these L2 protein extracts revealed that RNAi-knockdown of PFK1, LDH or
329 PDH did not affect Akt or dS6K phosphorylation (Figure 4C). In contrast, PK knockdown
330 strongly decreased dS6K phosphorylation and to a lower extent Akt phosphorylation
331 (Figure 4C). These results indicate that mTORC1 signaling may be affected when
332 knocking down PK, but not when knocking down any other enzyme directly linked to
333 glycolysis. Nonetheless, the lethal phenotype of PK-RNAi larvae occurring at the late L2
334 stage (Figure 4B) might weaken the larvae, inducing a subsequent effect on mTOR
335 signaling.

336 To evaluate the requirement of glycolysis for adult survival, RNAi-knockdown was
337 induced by temperature shift to 29°C in newly emerged flies and lethality was counted
338 every second day. In both males and females, PK and PFK1 knockdown provoked
339 lethality between 10 to 14 days after temperature shift (Figure 4D). Knockdown of PDH
340 and LDH also induced adult lethality, although not as soon as PK and PFK1 knockdown

(Figure 4D). As a comparison, to evaluate the consequence of disrupting fatty acid synthesis, we knocked-down FASN (Fatty Acid Synthase, Figure 4A) in adults; about a quarter of *FASN-RNAi* flies died between 10 to 14 days, while the others survived nearly as well as control flies (Figure 4D). Taken together, these data indicate that glycolysis is essential for both larval development and adult survival. However, prior to the appearance of the deleterious phenotype, glycolysis knockdown is unlikely to impinge on mTOR signaling.

Cell-autonomous requirement of glycolysis for Ilp- but not mTORC1-dependent overgrowth

To investigate the requirement of glycolysis to sustain cell-autonomous overgrowth dependent on Ilp- and mTORC1-signaling, *PFK1-RNAi*, *PK-RNAi*, *PDH-RNAi* and *LDH-RNAi* were induced in *PTEN*$^{-/-}$ or *Rheb*$^{+}$ clones. Except a moderate effect of *PK-RNAi*, clones expressing interfering RNA against these metabolic enzymes did not significantly affect the growth of FB cells (Figure 5A-D and 5M). In combined clones, none of the RNAi affected the growth of *Rheb*$^{+}$ clones (Figure 5E-H and 5M). In contrast, the size of *PTEN*$^{-/-}$ clones was significantly decreased when co-expressing RNAi against any of these metabolic enzymes (Figure 5I-M). These findings indicate that both aerobic and anaerobic glycolysis are required to sustain cell-autonomous overgrowth dependent on Ilp signaling. In contrast, reducing glycolysis does not counteract cell-autonomous overgrowth dependent on mTORC1 signaling, suggesting the existence of compensatory pathways.

Linking Lipogenesis to mTORC1- and Ilp-signaling

Since glycolysis and FA synthesis are tightly connected metabolic pathways (GARRIDO *et al.* 2015), we investigated whether lipogenesis affects Ilp or mTORC1 signaling. FA synthesis is catalyzed by FASN (Figure 4A). The *Drosophila* genome encodes three *FASN* genes, *FASN1* is ubiquitously expressed but not *FASN2* or *FASN3* (PARVY *et al.* 2012; CHUNG *et al.* 2014; WICKER-THOMAS *et al.* 2015). The deletion of the *FASN1* and *FASN2* tandem ($FASN^{\Delta 24\text{-}23}$ deletion, hereafter called $FASN^{1\text{-}2}$) results in a lethal phenotype that can be rescued by feeding larvae a lipid-complemented diet (beySD) (GARRIDO *et al.* 2015; WICKER-THOMAS *et al.* 2015). We observed that beySD-rescued $FASN^{1\text{-}2}$ mutant larvae exhibited a delay in development, as measured by the duration of larval development to metamorphosis entry (Figure 6A). Further, when beySD-rescued $FASN^{1\text{-}2}$ mutant larvae were transferred at the L2/L3 larval transition onto a 10% sucrose-supplemented-beySD, only a few of them completed the third larval stage and, after an extreme developmental delay, entered metamorphosis (Figure 6A). Delay in development can be due to a default in ecdysone production that results in giant pupae (PARVY *et al.* 2014) or to impaired mTOR signaling that results in reduced body growth (MONTAGNE *et al.* 1999; OLDHAM *et al.* 2000). Measurements of prepupal weight revealed that $FASN^{1\text{-}2}$ mutant prepupae exhibited a severe reduction in body weight, whether or not they were supplemented with sucrose (Figure 6B), suggesting a default in mTOR signaling. Therefore, we analyzed the phosphorylation of the *Drosophila* S6Kinase (dS6K) and Akt in protein extracts of late feeding L3 larvae. Western-blotting revealed that the dS6K protein resolved in several bands in $FASN^{1\text{-}2}$ extracts, whereas Akt protein was unchanged (Figure 6C). These results suggest that dS6K but not Akt might be degraded in the $FASN^{1\text{-}2}$ mutant background. In addition, dS6K phosphorylation decreased in $FASN^{1\text{-}2}$ extracts and became barely detectable when $FASN^{1\text{-}2}$ larvae were fed a sucrose-supplemented-beySD (Figure 6C). Conversely, the

phosphorylation of Akt was unaffected in larvae fed a beySD, although it was slightly decreased in larvae fed a sucrose-supplemented-beySD (Figure 6C). This finding contrasts with our previous observation showing that FB explants of *FASN*$^{1-2}$ mutant larvae were hypersensitive to insulin (GARRIDO *et al.* 2015). However, *FASN*$^{1-2}$ mutants also exhibited a decrease in food intake (GARRIDO *et al.* 2015), which might induce a systemic suppression of dS6K phosphorylation, while FB explant were cultured in nutrient media supplemented with insulin. Therefore, to determine whether *FASN* mutation affects mTOR signaling at the cell-autonomous level, we analyzed P-S6 and P-Akt in *FASN*$^{1-2}$ mutant clones in the FB. As for control clones, about half of the *FASN*$^{1-2}$ clonal cells were P-S6 positive (Figure 2J and 2K). Furthermore, no effect on P-Akt was observed in *FASN*$^{1-2}$ clonal cells (Figure 2D). In summary, these findings reveal that disrupting FA synthesis does not significantly affect mTORC1 and Ilp signaling at the cell-autonomous level, although it seems to impinge on mTORC1 signaling when inhibited in the whole animal whether directly or indirectly.

Cell-autonomous requirement of FA synthesis for Ilp- but not mTORC1-dependent overgrowth

To determine, whether lipogenesis is required at the cell-autonomous level to sustain mTORC1 and/or Ilp dependent growth, we analyzed *FASN*$^{1-2}$ clones while enhancing either of the mTOR signaling branch in FB cells. We previously reported (GARRIDO *et al.* 2015) that *FASN*$^{1-2}$ clonal cells in the FB were slightly reduced in size and that this effect was dramatically increased in larvae fed a 20%-SSD (Figure S1 and Figure 7M). Therefore, we generated *PTEN*$^{-/-}$ and *Rheb*$^{+}$ clones combined or not with the *FASN*$^{1-2}$ mutation and analyzed them in the FB of larvae fed either a standard diet or a 20%-SSD. As compared to the standard diet, feeding larvae a 20%-SSD had no effect on the

size of *Rheb*$^{+}$ clonal cells, but significantly reduced the size of *PTEN*$^{-/-}$ and of *PTEN*$^{-/-}$;*Rheb*$^{+}$ clonal cells (Figure 7A-F and 7M). Further, when combined with the *FASN*$^{1-2}$ mutation, *PTEN*$^{-/-}$ but not *Rheb*$^{+}$ clones were significantly reduced in size (Figure 7G-H and 7M). The *FASN*$^{1-2}$ mutation also provoked a severe size reduction of *PTEN*$^{-/-}$,*Rheb*$^{+}$ clones (Figure 7I and 7M). Moreover, as compared to the standard diet, feeding larvae a 20%-SSD induced a significant size reduction of *FASN*$^{1-2}$;*Rheb*$^{+}$, *FASN*$^{1-2}$,*PTEN*$^{-/-}$ and *FASN*$^{1-2}$,*PTEN*$^{-/-}$;*Rheb*$^{+}$ clonal cells (Figure 7J-L and 7M). Of note, except for the *FASN*$^{1-2}$;*Rheb*$^{+}$ clonal cells in larvae fed a 20%-SSD that exhibited a size roughly identical to that of the surrounding control cells (Figure 7J), the cell size was always bigger than the controls (Figure 7M). These findings indicate that, in larvae fed a standard diet, FA synthesis is at least in part required to sustain over-growth induced by Ilp, but not mTORC1. They also reveal that additional dietary sucrose is rather detrimental for the growth of cells either deficient for FA synthesis or over-active for Ilp signaling, suggesting that these cells have a restricted homeostatic ability to adjust to an unbalanced diet, whereas mTORC1 activated cells at least in part maintain this ability.

DISCUSSION

In this study, we used the powerful *Drosophila* genetics to investigate the functional links between the glycolytic/lipogenic axis and mTORC1- or Ilp-dependent growth. In agreement with previous studies (RADIMERSKI *et al.* 2002a; RADIMERSKI *et al.* 2002b; DONG AND PAN 2004; MONTAGNE *et al.* 2010; PALLARES-CARTES *et al.* 2012), we show that mTORC1 and Ilp signaling work independently in the *Drosophila* FB. Further, we provide evidence that the previously described *mTOR*^{2L1} mutation that likely results in a kinase-inactive protein (OLDHAM *et al.* 2000) affects mTORC1 but not Ilp signaling.

Congruently, a study on a *Drosophila rictor* mutant reported that the mTORC2 complex was not required to sustain Akt-dependent growth, but rather to play as a rheostat for this signaling branch (HIETAKANGAS AND COHEN 2007). Although this study suggests that mTOR is dispensable for Akt activity, we show that Akt activity and Ilp-dependent overgrowth are suppressed in *mTOR*$^{\Delta P}$ mutant indicating that the mTOR protein is required for these processes.

On one hand, to mimic the effect that might be induced by drug treatment with a systemic inhibitor, we dampened the glycolytic/lipogenic axis or enhanced mTORC1 or Ilp signaling in the entire organism. On the other hand, to monitor the cell growth process that spans the entire developmental program at the cell-autonomous level, we analyzed clonal FB cells in mosaic animals. Intriguingly, our study reveals apparent contradictory effects between perturbations at the whole body and cell-autonomous levels. At the organismal level, knockdown of glycolytic enzymes or deficiency of FASN result in animal lethality. However, *FASN*$^{1\text{-}2}$ mutant animals supplemented with dietary lipids can survive but exhibit a dramatic overall growth suppression. This growth defect might result from a decrease in mTORC1 activity that is strongly reduced in *FASN*$^{1\text{-}2}$ mutant animals, suggesting that mTORC1 but not Ilp signaling relies on lipogenesis. In contrast, at the cell autonomous level, the mutation of *FASN*$^{1\text{-}2}$ restrains Ilp but not mTORC1 dependent overgrowth in FB cells. These apparent contradictory findings, suggest that the growth defect and the reduction of mTORC1 activity in *FASN*$^{1\text{-}2}$ mutants are not due to the addition of cell-autonomous effects but rather to a systemic regulation. Potentially, FASN default might affect the activity of a specific tissue, as for instance, the neurosecretory cells that synthesize and secrete Ilps, which promote systemic body growth (RULIFSON *et al.* 2002). Alternatively, considering that mTORC1 directly responds to nutrients (DIBBLE AND MANNING 2013; GROENEWOUD AND

ZWARTKRUIS 2013; MONTAGNE 2016), the drop of mTORC1 activity may be a consequence of feeding, since we previously reported a decrease in nutrient uptake in *FASN*$^{1-2}$ mutant animals (GARRIDO *et al.* 2015). Consistently, a previous study on the transcription factor Mondo —the *Drosophila* homologue of mondoA and ChREBP that regulate the glycolytic/lipogenic axis in response to dietary sugar (MATTILA *et al.* 2015; RICHARDS *et al.* 2017)— suggests the existence of a FASN-dependent effect in the FB on the control of food intake (SASSU *et al.* 2012). FB-knockdown of *mondo* results in the lack of sucrose-induced expression of *FASN1* and in a decrease in food intake. This study suggests that the FASN default perturbs body homeostasis and indirectly affects the neuronal control of feeding behavior. However, it does not exclude that a lipogenic defect in neuronal cells may also directly impinge on feeding behavior. Finally, the drop of mTORC1 activity observed in *FASN*$^{1-2}$ mutants may be a consequence of malonyl-CoA accumulation, since mTOR malonylation has been reported to inhibit mTORC1- but not Ilp/mTORC2-dependent activity (BRUNING *et al.* 2018). Malonylation of mTOR may also account for the size reduction of *FASN*$^{1-2}$ mutant cells over-expressing Rheb in animals fed a 20%-SSD, consistent with the increased expression of lipogenic enzymes induced by dietary sucrose (GARRIDO *et al.* 2015). Thus, mTOR malonylation and the subsequent decrease in mTORC1 activity might occur only when interfering with a context of high demand for lipogenesis, an issue that should be investigated in the future.

Our study reveals that over-activation of mTORC1 and to a lesser extent of Ilp signaling, results in a decrease in glycogen and TAG stores and in circulating trehalose, suggesting that activation of either signaling branch enhances metabolite consumption to sustain cell growth. It is therefore surprising that activation of neither mTORC1 nor Ilp signaling induces an increase in body weight. Nonetheless, overall body growth

depends on an intricate regulatory network that integrates cell-autonomous effects and humoral messages. For instance, previous studies reported that activation of Ilp signaling within the ring gland, results in a systemic decrease in body growth (CALDWELL *et al.* 2005; COLOMBANI *et al.* 2005; MIRTH 2005). Therefore, ubiquitous activation of mTORC1 or Ilp signaling is likely to promote the growth of most cells but might concurrently perturb endocrine signals dampening overall growth. Of note, we observed that larvae fed a 20%-SSD result in pupae with reduced body weight, an effect that is partially suppressed when either mTORC1 or Ilp signaling is over-activated. The fact that the overall body weight of these animals is maintained within a range likely compatible with organismal survival contrasts with the observed high rate of lethality. The decrease in stores and circulating sugars suggests that in these animals each cell tends to increase its basal metabolism evoking an egoist behavior that might perturb the equilibrium between cell-autonomous and systemic regulation. Thus, in a stressful situation, as when animals are fed a 20%-SSD, the need of a tight adjustment to an unbalanced diet may enhance the distortion between cell-autonomous effects and systemic regulation, resulting in an increased rate of lethality.

A plethora of studies in mammalian cells indicate that mTOR activation directs metabolism towards glucose consumption, storage and anabolism (GOTTLOB *et al.* 2001; INOKI *et al.* 2003b; HAHN-WINDGASSEN *et al.* 2005; DUVEL *et al.* 2010; PETERSON *et al.* 2011; HOUDDANE *et al.* 2017; JALDIN-FINCATI *et al.* 2017; WIPPERMAN *et al.* 2019). Our study rather suggests that in the *Drosophila* larvae, mTOR promotes metabolite consumption through glycolysis but not storage. However, at the cell-autonomous level, we observe that inhibition of lipogenesis or glycolysis restrains neither larval FB cell growth nor overgrowth induced by mTORC1 stimulation in these cells. These findings counteract the idea that mTORC1 potentiates a glycolytic/lipogenic axis (DUVEL *et al.*

2010) to sustain cell growth. To overcome the lack of glycolytic products and of membrane lipids, these cells may benefit of a transfer from neighboring cells and might favor alternative metabolic pathways, including glutamine catabolism to feed TCA anaplerosis, which has been shown to be a crucial pathway in mTORC1-stimulated mammalian cells (CHOO *et al.* 2010; CSIBI *et al.* 2013; CSIBI *et al.* 2014). Nonetheless, such compensatory processes do not fully operate to sustain Ilp-dependent overgrowth. In these cells, the mutation of PTEN potentially impedes the ability to modulate this signaling branch. Therefore, it is tempting to speculate that the modulation of Ilp signaling at least in part contributes to the regulation of these compensatory processes.

As a coordinator of growth and metabolism, mTOR plays a central role in tumor development (DOWLING *et al.* 2010; HARACHI *et al.* 2018; MOSSMANN *et al.* 2018; TIAN *et al.* 2019). PTEN, the tumor suppressor that counteracts PI3K activity downstream of the Ilp receptor, is deficient in several human cancers (CULLY *et al.* 2006). Mutation of TSC1 or TSC2, which results in mTORC1 hyper-activation, is associated with benign tumors but also with brain, kidney and lung destructive diseases (HENSKE *et al.* 2016). To investigate the role of mTOR regarding tumor development, a recent study reported the generation of liver-specific double knockout mice for TSC1 and PTEN (GURI *et al.* 2017). These mice develop hepatic steatosis that eventually progresses to hepatocellular carcinoma. Both processes are suppressed in mice fed the mTORC1/2 inhibitors INK128, but not the mTORC1 inhibitor rapamycin, supporting an Ilp/mTORC2 specific effect. The combination of inhibitors against mTOR and metabolism is currently under clinical investigation to fight cancers (MOSSMANN *et al.* 2018). Importantly, our study reveals that ubiquitous inhibition of basal metabolism produces dramatic effects during development, while at the cell-autonomous level, it only moderates growth induced by over-activation of Ilp/mTORC2 signaling. Therefore, the use of drug therapy

to fight cancer must be taken with caution, in particular if organismal development is not complete and most efforts should be made to selectively target sick tissues.

AKNOWLEDGMENTS

We wish to thank D Petit for preparing the fly media, H Stocker for fly stocks, A Teleman for the phospho-S6 antibody, M Gettings for editing the manuscript, and the NIG and VDRC stock centers for RNAi fly strains. We wish to thank the *French government* for fellowship to MD (MENRT 2015-155) and DG (MRT 2011-78), the *Fondation pour la Recherche Médicale* for fellowship to DG (FDT201 4093 0800), the *Fondation ARC* for grant support to JM (projet ARC 1555286) and the *Ligue de Recherche contre le Cancer* for grant support to JM (M27218). The authors declare no competing financial interests.

AUTHOR CONTRIBUTIONS

JM designed the experiments; MD, DG, MP, TR and JM performed the experiments; MD, DG, ALR and JM analyzed the results; and JM wrote the manuscript.

FIGURE LEGENDS

Figure 1: mTORC1- and Ilp-dependent growth in FB cells. (**A-L**) MARCM clones labeled by GFP (green) in the FB of L3 larvae. Nuclei were labeled with DAPI (silver) and membranes with phalloidin (red). Control (A), *Rheb*$^{+}$ (B), *PTEN*$^{-/-}$ (C) and *PTEN*$^{-/-}$;*Rheb*$^{+}$ (D) clones were generated in a wild type background. *Rheb*$^{+}$ (E), *PTEN*$^{-/-}$ (F), *mTOR*^{2L1} (G) *mTOR*^{2L1}, *Rheb*$^{+}$ (H) *mTOR*^{2L1},*PTEN*$^{-/-}$ (I), *mTOR*$^{\Delta P}$ (J), *mTOR*$^{\Delta P}$,*Rheb*$^{+}$

563 (K) and *mTOR*$^{\Delta P}$,*PTEN*$^{-/-}$ (L) clones were generated in a *Minute* (*M*) background. Scale
564 bars: 50µm. (**M**) Relative size of control (Co), *Rheb*$^{+}$, *PTEN*$^{-/-}$, and *PTEN*$^{-/-}$;*Rheb*$^{+}$ clonal
565 cells generated in a wild type background.

566

567 **Figure 2: mTORC1 and Ilp signaling activity in FB cells.** (**A-J**) MARCM clones
568 labeled by GFP (green) in the FB of L3 larvae. Clones were generated in a wild type
569 (A,D,E,H,I,J) or a *Minute* (B,C,F,G) background and nuclei were labeled with DAPI
570 (silver). FB tissues with *PTEN*$^{-/-}$ (A), *mTOR*$^{\Delta P}$ (B), *mTOR*^{2L1} (C) and *FASN*$^{1-2}$ (D) clones
571 were stained with a phospho-AKT antibody. FB tissues with control (E), *mTOR*^{2L1} (F),
572 *mTOR*$^{\Delta P}$ (G) *Rheb*$^{+}$ (H), *PTEN*$^{-/-}$ (I) and *FASN*$^{1-2}$ (J) clones were stained with a
573 phospho-S6 antibody. Scale bars: 50µm. (**K**) Percentage of P-S6 positive clones with
574 respect to the total number of MARCM clones for control, *FASN*$^{1-2}$, *PTEN*$^{-/-}$, *Rheb*$^{+}$,
575 *mTOR*^{2L1} and *mTOR*$^{\Delta P}$ genotypes.

576

577 **Figure 3: Enhanced mTORC1 or Ilp signaling affects larval metabolism.** (**A-B**)
578 Body weight of female (A) and male (B) prepupae formed from larvae fed either a
579 standard (0%) or a 20%-SSD (20%) as from the L2/L3 transition. (**C-F**) Measurement of
580 total protein (C), TAG (D), glycogen (E) and trehalose (F) levels in prepupae fed either a
581 standard or a 20%-SSD. Prepupae used in these measurements were the F1 progeny
582 from *da-gal4* virgin females mated to either control (Co), *EP(UAS)-Rheb* (*Rheb*$^{++}$) or
583 *UAS-PTEN-RNAi* (*PTEN-Ri*) males.

584

585 **Figure 4: Glycolysis knockdown in whole organisms.** (**A**) Scheme of basal
586 metabolism. Glucose and trehalose enter glycolysis as glucose-6P, whereas fructose

follows a distinct pathway to triose-P. Enzymes investigated in the present study are marked in red. (**B**) Phenotype of ubiquitous RNAi knockdown of PFK1, PK, LDH and PDH. Flies were left to lay eggs overnight either at 29°C (column 0h) or at 19°C and transferred to 29°C the day after (column 24h); then development proceeded at 29°C (i.e. the temperature that inactivates Gal80). (**C**) Western-blot analysis of total (top) or phosphorylated (mid) dS6K (left) or Akt (right) proteins; tubulin (bottom) was used as a loading control. Protein extracts were prepared with late L2 control larvae (Co) or L2 larvae expressing RNAi against the indicated metabolic enzymes. (**E-F**) Survival at 29°C of male (top) and female (bottom) control flies or flies expressing RNAi against the indicated metabolic enzymes as from adult eclosion.

Figure 5: Cell-autonomous requirement of glycolysis for Ilp- but not mTORC1-dependent overgrowth. (**A-G**) MARCM clones labeled by GFP (green) in the FB of L3 larvae. Nuclei were labeled with DAPI (silver) and membranes with phalloidin (red). Genotypes of MARCM clones are: *PFK1-RNAi* (A), *PK-RNAi* (B), *LDH-RNAi* (C), *PDH-RNAi* (D), *Rheb*$^{+}$,*PFK1-RNAi* (E), *Rheb*$^{+}$,*PK-RNAi* (F), *Rheb*$^{+}$,*LDH-RNAi* (G), *Rheb*$^{+}$,*PDH-RNAi* (H), *PTEN*$^{-/-}$;*PFK1-RNAi* (I), *PTEN*$^{-/-}$;*PK-RNAi* (J), *PTEN*$^{-/-}$;*PDH-RNAi* (K) and *PTEN*$^{-/-}$;*PDH-RNAi* (L). Scale bars: 50µm. (**M**) Relative size of clonal cells corresponding to the clones shown in A-L, and in Figure 1A for control (Co).

Figure 6: *FASN*$^{1-2}$ mutation affects developmental growth and mTORC1 signaling. (**A**) Developmental duration from egg laying to metamorphosis onset of *w*^{1118} control (Co) and *FASN*$^{1-2}$ (FASN) larvae fed either a beySD (0%) or a 10% sucrose-supplemented-beySD as from the L2/L3 transition (10%); n: total number of larvae collected for each condition. (**B**) Prepupal weight of females (left) and males (right) as

612 listed in 6A; the numbers of weighted prepupae are indicated above each sample. (**C**)
613 Western-blot analysis of (from top to bottom) total dS6K, phosphorylated dS6K, total
614 Akt, phosphorylated Akt and total tubulin as a loading control. Protein extracts were
615 prepared from feeding L3 larvae prior to the wandering stage as listed in 6A. For each
616 condition, at least 30 larvae were used to prepare protein extracts.

617

618 **Figure 7: Cell-autonomous requirement of FASN activity for Ilp- but not mTORC1-**
619 **dependent overgrowth.** (**A-L**) MARCM clones labeled by GFP (green) in the FB of L3
620 larvae fed either a standard (A-C, G-I) or a 20%-SSD (D-F, J-L). Nuclei were labeled
621 with DAPI (silver) and membranes with phalloidin (red). Genotypes of MARCM clones
622 are: *Rheb*$^{+}$ (A,D), *PTEN*$^{-/-}$ (B,E) *PTEN*$^{-/-}$,*Rheb*$^{+}$ (C,F), *FASN*$^{1-2}$;*Rheb*$^{+}$ (G,J) *FASN*$^{1-}$
623 ^{2},*PTEN*$^{-/-}$ (H,K) and the *FASN*$^{1-2}$,*PTEN*$^{-/-}$;*Rheb*$^{+}$ (I,L). Scale bars: 50µm. (**M**) Relative
624 size of clonal cells corresponding to the clones shown in A-L and in Figure S1 for
625 *FASN*$^{1-2}$ and Figure 1A for control (Co).

626

627 **LITERATURE CITED**

628 Antikainen, H., M. Driscoll, G. Haspel and R. Dobrowolski, 2017 TOR-mediated
629 regulation of metabolism in aging. Aging Cell 16**:** 1219-1233.

630 Bates, D., M. Mächler, B. M. Bolker and S. Walker, 2015 Fitting Linear Mixed-Effects
631 Models Using lme4. Journal of Statistical Software 67**:** 1-48.

632 Bohni, R., J. Riesgo-Escovar, S. Oldham, W. Brogiolo, H. Stocker *et al.*, 1999
633 Autonomous control of cell and organ size by CHICO, a Drosophila homolog of
634 vertebrate IRS1-4. Cell 97**:** 865-875.

635 Bruning, U., F. Morales-Rodriguez, J. Kalucka, J. Goveia, F. Taverna *et al.*, 2018
636 Impairment of Angiogenesis by Fatty Acid Synthase Inhibition Involves mTOR
637 Malonylation. Cell Metab 28**:** 866-880 e815.

638 Caldwell, P. E., M. Walkiewicz and M. Stern, 2005 Ras activity in the Drosophila
639 prothoracic gland regulates body size and developmental rate via ecdysone
640 release. Curr Biol 15**:** 1785-1795.

641 Caron, A., D. Richard and M. Laplante, 2015 The Roles of mTOR Complexes in Lipid
642 Metabolism. Annu Rev Nutr 35**:** 321-348.

643 Choo, A. Y., S. G. Kim, M. G. Vander Heiden, S. J. Mahoney, H. Vu *et al.*, 2010
644 Glucose addiction of TSC null cells is caused by failed mTORC1-dependent
645 balancing of metabolic demand with supply. Mol Cell 38**:** 487-499.

646 Chung, H., D. W. Loehlin, H. D. Dufour, K. Vaccarro, J. G. Millar *et al.*, 2014 A single
647 gene affects both ecological divergence and mate choice in Drosophila. Science
648 343**:** 1148-1151.

649 Colombani, J., L. Bianchini, S. Layalle, E. Pondeville, C. Dauphin-Villemant *et al.*, 2005
650 Antagonistic actions of ecdysone and insulins determine final size in Drosophila.
651 Science 310**:** 667-670.

652 Csibi, A., S. M. Fendt, C. Li, G. Poulogiannis, A. Y. Choo *et al.*, 2013 The mTORC1
653 pathway stimulates glutamine metabolism and cell proliferation by repressing
654 SIRT4. Cell 153**:** 840-854.

655 Csibi, A., G. Lee, S. O. Yoon, H. Tong, D. Ilter *et al.*, 2014 The mTORC1/S6K1 pathway
656 regulates glutamine metabolism through the eIF4B-dependent control of c-Myc
657 translation. Curr Biol 24**:** 2274-2280.

Cully, M., H. You, A. J. Levine and T. W. Mak, 2006 Beyond PTEN mutations: the PI3K pathway as an integrator of multiple inputs during tumorigenesis. Nat Rev Cancer 6**:** 184-192.

Dibble, C. C., W. Elis, S. Menon, W. Qin, J. Klekota *et al.*, 2012 TBC1D7 is a third subunit of the TSC1-TSC2 complex upstream of mTORC1. Mol Cell 47**:** 535-546.

Dibble, C. C., and B. D. Manning, 2013 Signal integration by mTORC1 coordinates nutrient input with biosynthetic output. Nat Cell Biol 15**:** 555-564.

Dietzl, G., D. Chen, F. Schnorrer, K. C. Su, Y. Barinova *et al.*, 2007 A genome-wide transgenic RNAi library for conditional gene inactivation in Drosophila. Nature 448**:** 151-156.

Dong, J., and D. Pan, 2004 Tsc2 is not a critical target of Akt during normal Drosophila development. Genes Dev 18**:** 2479-2484.

Dowling, R. J., I. Topisirovic, B. D. Fonseca and N. Sonenberg, 2010 Dissecting the role of mTOR: lessons from mTOR inhibitors. Biochim Biophys Acta 1804**:** 433-439.

Duvel, K., J. L. Yecies, S. Menon, P. Raman, A. I. Lipovsky *et al.*, 2010 Activation of a metabolic gene regulatory network downstream of mTOR complex 1. Mol Cell 39**:** 171-183.

Edgar, B. A., and T. L. Orr-Weaver, 2001 Endoreplication cell cycles: more for less. Cell 105**:** 297-306.

Engelman, J. A., J. Luo and L. C. Cantley, 2006 The evolution of phosphatidylinositol 3-kinases as regulators of growth and metabolism. Nat Rev Genet 7**:** 606-619.

679 Garami, A., F. J. Zwartkruis, T. Nobukuni, M. Joaquin, M. Roccio *et al.*, 2003 Insulin
680 activation of Rheb, a mediator of mTOR/S6K/4E-BP signaling, is inhibited by
681 TSC1 and 2. Mol Cell 11**:** 1457-1466.

682 Garrido, D., T. Rubin, M. Poidevin, B. Maroni, A. Le Rouzic *et al.*, 2015 Fatty Acid
683 Synthase Cooperates with Glyoxalase 1 to Protect against Sugar Toxicity. PLoS
684 Genet 11**:** e1004995.

685 Goberdhan, D. C., M. H. Ogmundsdottir, S. Kazi, B. Reynolds, S. M. Visvalingam *et al.*,
686 2009 Amino acid sensing and mTOR regulation: inside or out? Biochem Soc Trans
687 37**:** 248-252.

688 Gottlob, K., N. Majewski, S. Kennedy, E. Kandel, R. B. Robey *et al.*, 2001 Inhibition of
689 early apoptotic events by Akt/PKB is dependent on the first committed step of
690 glycolysis and mitochondrial hexokinase. Genes Dev 15**:** 1406-1418.

691 Groenewoud, M. J., and F. J. Zwartkruis, 2013 Rheb and mammalian target of
692 rapamycin in mitochondrial homoeostasis. Open Biol 3**:** 130185.

693 Guri, Y., M. Colombi, E. Dazert, S. K. Hindupur, J. Roszik *et al.*, 2017 mTORC2
694 Promotes Tumorigenesis via Lipid Synthesis. Cancer Cell 32**:** 807-823 e812.

695 Haeusler, R. A., T. E. McGraw and D. Accili, 2018 Biochemical and cellular properties of
696 insulin receptor signalling. Nat Rev Mol Cell Biol 19**:** 31-44.

697 Hagiwara, A., M. Cornu, N. Cybulski, P. Polak, C. Betz *et al.*, 2012 Hepatic mTORC2
698 activates glycolysis and lipogenesis through Akt, glucokinase, and SREBP1c. Cell
699 Metab 15**:** 725-738.

700 Hahn-Windgassen, A., V. Nogueira, C. C. Chen, J. E. Skeen, N. Sonenberg *et al.*, 2005
701 Akt activates the mammalian target of rapamycin by regulating cellular ATP level
702 and AMPK activity. J Biol Chem 280**:** 32081-32089.

703 Harachi, M., K. Masui, Y. Okamura, R. Tsukui, P. S. Mischel *et al.*, 2018 mTOR
704 Complexes as a Nutrient Sensor for Driving Cancer Progression. Int J Mol Sci 19.

705 Hay, N., and N. Sonenberg, 2004 Upstream and downstream of mTOR. Genes Dev 18**:**
706 1926-1945.

707 Henske, E. P., S. Jozwiak, J. C. Kingswood, J. R. Sampson and E. A. Thiele, 2016
708 Tuberous sclerosis complex. Nat Rev Dis Primers 2**:** 16035.

709 Hietakangas, V., and S. M. Cohen, 2007 Re-evaluating AKT regulation: role of TOR
710 complex 2 in tissue growth. Genes Dev 21**:** 632-637.

711 Holm, S., 1079 A simple sequentially rejective multiple test procedure. Scand J Statist
712 6.

713 Hothorn, T., F. Bretz and P. Westfall, 2008 Simultaneous inference in general
714 parametric models. Biom J 50**:** 346-363.

715 Houddane, A., L. Bultot, L. Novellasdemunt, M. Johanns, M. A. Gueuning *et al.*, 2017
716 Role of Akt/PKB and PFKFB isoenzymes in the control of glycolysis, cell
717 proliferation and protein synthesis in mitogen-stimulated thymocytes. Cell Signal
718 34**:** 23-37.

719 Howell, J. J., S. J. Ricoult, I. Ben-Sahra and B. D. Manning, 2013 A growing role for
720 mTOR in promoting anabolic metabolism. Biochem Soc Trans 41**:** 906-912.

721 Inoki, K., Y. Li, T. Xu and K. L. Guan, 2003a Rheb GTPase is a direct target of TSC2
722 GAP activity and regulates mTOR signaling. Genes Dev 17**:** 1829-1834.

723 Inoki, K., T. Zhu and K. L. Guan, 2003b TSC2 mediates cellular energy response to
724 control cell growth and survival. Cell 115**:** 577-590.

725 Jaldin-Fincati, J. R., M. Pavarotti, S. Frendo-Cumbo, P. J. Bilan and A. Klip, 2017
726 Update on GLUT4 Vesicle Traffic: A Cornerstone of Insulin Action. Trends
727 Endocrinol Metab 28**:** 597-611.

728 Kim, D. H., D. D. Sarbassov, S. M. Ali, J. E. King, R. R. Latek *et al.*, 2002 mTOR
729 interacts with raptor to form a nutrient-sensitive complex that signals to the cell
730 growth machinery. Cell 110**:** 163-175.

731 Lamming, D. W., and D. M. Sabatini, 2013 A Central role for mTOR in lipid
732 homeostasis. Cell Metab 18**:** 465-469.

733 Laplante, M., and D. M. Sabatini, 2012 mTOR signaling in growth control and disease.
734 Cell 149**:** 274-293.

735 Lee, T., and L. Luo, 2001 Mosaic analysis with a repressible cell marker (MARCM) for
736 Drosophila neural development. Trends Neurosci 24**:** 251-254.

737 Lehmann, M., 2018 Endocrine and physiological regulation of neutral fat storage in
738 Drosophila. Mol Cell Endocrinol 461**:** 165-177.

739 Lien, E. C., C. C. Dibble and A. Toker, 2017 PI3K signaling in cancer: beyond AKT. Curr
740 Opin Cell Biol 45**:** 62-71.

741 Ma, X. M., and J. Blenis, 2009 Molecular mechanisms of mTOR-mediated translational
742 control. Nat Rev Mol Cell Biol 10**:** 307-318.

743 Magnuson, B., B. Ekim and D. C. Fingar, 2012 Regulation and function of ribosomal
744 protein S6 kinase (S6K) within mTOR signalling networks. Biochem J 441**:** 1-21.

745 Majewski, N., V. Nogueira, P. Bhaskar, P. E. Coy, J. E. Skeen *et al.*, 2004 Hexokinase-
746 mitochondria interaction mediated by Akt is required to inhibit apoptosis in the
747 presence or absence of Bax and Bak. Mol Cell 16**:** 819-830.

748 Mattila, J., E. Havula, E. Suominen, M. Teesalu, I. Surakka *et al.*, 2015 Mondo-Mlx
749 Mediates Organismal Sugar Sensing through the Gli-Similar Transcription Factor
750 Sugarbabe. Cell Rep 13**:** 350-364.

751 McManus, E. J., K. Sakamoto, L. J. Armit, L. Ronaldson, N. Shpiro *et al.*, 2005 Role that
752 phosphorylation of GSK3 plays in insulin and Wnt signalling defined by knockin
753 analysis. EMBO J 24**:** 1571-1583.

754 Mirth, C., 2005 Ecdysteroid control of metamorphosis in the differentiating adult leg
755 structures of Drosophila melanogaster. Dev Biol 278**:** 163-174.

756 Montagne, J., 2016 A Wacky Bridge to mTORC1 Dimerization. Dev Cell 36**:** 129-130.

757 Montagne, J., C. Lecerf, J. P. Parvy, J. M. Bennion, T. Radimerski *et al.*, 2010 The
758 nuclear receptor DHR3 modulates dS6 kinase-dependent growth in Drosophila.
759 PLoS Genet 6**:** e1000937.

760 Montagne, J., T. Radimerski and G. Thomas, 2001 Insulin signaling: lessons from the
761 Drosophila tuberous sclerosis complex, a tumor suppressor. Sci STKE 2001**:**
762 PE36.

763 Montagne, J., M. J. Stewart, H. Stocker, E. Hafen, S. C. Kozma *et al.*, 1999 Drosophila
764 S6 kinase: a regulator of cell size. Science 285**:** 2126-2129.

765 Montagne, J., and G. Thomas, 2004 S6K integrates nutrient and mitogen signals to
766 control cell growth. , pp. 265-298 in *Cell growth: control of cell size.*, edited by M.
767 Hall, Raff, M., Thomas, G. Cold Spring Harbor Press.

768 Morata, G., and P. Ripoll, 1975 Minutes: mutants of drosophila autonomously affecting
769 cell division rate. Dev Biol 42**:** 211-221.

770 Mossmann, D., S. Park and M. N. Hall, 2018 mTOR signalling and cellular metabolism
771 are mutual determinants in cancer. Nat Rev Cancer 18: 744-757.

772 Nakae, J., T. Kitamura, D. L. Silver and D. Accili, 2001 The forkhead transcription factor
773 Foxo1 (Fkhr) confers insulin sensitivity onto glucose-6-phosphatase expression. J
774 Clin Invest 108: 1359-1367.

775 Oldham, S., J. Montagne, T. Radimerski, G. Thomas and E. Hafen, 2000 Genetic and
776 biochemical characterization of dTOR, the Drosophila homolog of the target of
777 rapamycin. Genes Dev 14: 2689-2694.

778 Padmanabha, D., and K. D. Baker, 2014 Drosophila gains traction as a repurposed tool
779 to investigate metabolism. Trends Endocrinol Metab 25: 518-527.

780 Pallares-Cartes, C., G. Cakan-Akdogan and A. A. Teleman, 2012 Tissue-specific
781 coupling between insulin/IGF and TORC1 signaling via PRAS40 in Drosophila.
782 Dev Cell 22: 172-182.

783 Parvy, J. P., L. Napal, T. Rubin, M. Poidevin, L. Perrin *et al.*, 2012 Drosophila
784 melanogaster Acetyl-CoA-carboxylase sustains a fatty acid-dependent remote
785 signal to waterproof the respiratory system. PLoS Genet 8: e1002925.

786 Parvy, J. P., P. Wang, D. Garrido, A. Maria, C. Blais *et al.*, 2014 Forward and feedback
787 regulation of cyclic steroid production in Drosophila melanogaster. Development
788 141: 3955-3965.

789 Peterson, T. R., S. S. Sengupta, T. E. Harris, A. E. Carmack, S. A. Kang *et al.*, 2011
790 mTOR complex 1 regulates lipin 1 localization to control the SREBP pathway. Cell
791 146: 408-420.

792 Polak, P., N. Cybulski, J. N. Feige, J. Auwerx, M. A. Ruegg *et al.*, 2008 Adipose-specific
793 knockout of raptor results in lean mice with enhanced mitochondrial respiration.
794 Cell Metab 8**:** 399-410.

795 Radimerski, T., J. Montagne, M. Hemmings-Mieszczak and G. Thomas, 2002a Lethality
796 of Drosophila lacking TSC tumor suppressor function rescued by reducing dS6K
797 signaling. Genes Dev 16**:** 2627-2632.

798 Radimerski, T., J. Montagne, F. Rintelen, H. Stocker, J. van der Kaay *et al.*, 2002b
799 dS6K-regulated cell growth is dPKB/dPI(3)K-independent, but requires dPDK1.
800 Nat Cell Biol 4**:** 251-255.

801 Richards, P., S. Ourabah, J. Montagne, A. F. Burnol, C. Postic *et al.*, 2017
802 MondoA/ChREBP: The usual suspects of transcriptional glucose sensing;
803 Implication in pathophysiology. Metabolism 70**:** 133-151.

804 Robey, R. B., and N. Hay, 2009 Is Akt the "Warburg kinase"?-Akt-energy metabolism
805 interactions and oncogenesis. Semin Cancer Biol 19**:** 25-31.

806 Romero-Pozuelo, J., C. Demetriades, P. Schroeder and A. A. Teleman, 2017
807 CycD/Cdk4 and Discontinuities in Dpp Signaling Activate TORC1 in the Drosophila
808 Wing Disc. Dev Cell 42**:** 376-387 e375.

809 Rulifson, E. J., S. K. Kim and R. Nusse, 2002 Ablation of insulin-producing neurons in
810 flies: growth and diabetic phenotypes. Science 296**:** 1118-1120.

811 Sarbassov, D. D., D. A. Guertin, S. M. Ali and D. M. Sabatini, 2005 Phosphorylation and
812 regulation of Akt/PKB by the rictor-mTOR complex. Science 307**:** 1098-1101.

813 Sassu, E. D., J. E. McDermott, B. J. Keys, M. Esmaeili, A. C. Keene *et al.*, 2012
814 Mio/dChREBP coordinately increases fat mass by regulating lipid synthesis and
815 feeding behavior in Drosophila. Biochem Biophys Res Commun 426**:** 43-48.

816 Saxton, R. A., and D. M. Sabatini, 2017 mTOR Signaling in Growth, Metabolism, and
817 Disease. Cell 168**:** 960-976.

818 Shimobayashi, M., and M. N. Hall, 2014 Making new contacts: the mTOR network in
819 metabolism and signalling crosstalk. Nat Rev Mol Cell Biol 15**:** 155-162.

820 Stocker, H., T. Radimerski, B. Schindelholz, F. Wittwer, P. Belawat *et al.*, 2003 Rheb is
821 an essential regulator of S6K in controlling cell growth in Drosophila. Nat Cell Biol
822 5**:** 559-565.

823 Tian, T., X. Li and J. Zhang, 2019 mTOR Signaling in Cancer and mTOR Inhibitors in
824 Solid Tumor Targeting Therapy. Int J Mol Sci 20.

825 Ugur, B., K. Chen and H. J. Bellen, 2016 Drosophila tools and assays for the study of
826 human diseases. Dis Model Mech 9**:** 235-244.

827 Wangler, M. F., Y. Hu and J. M. Shulman, 2017 Drosophila and genome-wide
828 association studies: a review and resource for the functional dissection of human
829 complex traits. Dis Model Mech 10**:** 77-88.

830 Wicker-Thomas, C., D. Garrido, G. Bontonou, L. Napal, N. Mazuras *et al.*, 2015 Flexible
831 origin of hydrocarbon/pheromone precursors in Drosophila melanogaster. J Lipid
832 Res 56**:** 2094-2101.

833 Wipperman, M. F., D. C. Montrose, A. M. Gotto, Jr. and D. P. Hajjar, 2019 Mammalian
834 Target of Rapamycin: A Metabolic Rheostat for Regulating Adipose Tissue
835 Function and Cardiovascular Health. Am J Pathol 189**:** 492-501.

836 Yang, H., X. Jiang, B. Li, H. J. Yang, M. Miller *et al.*, 2017 Mechanisms of mTORC1
837 activation by RHEB and inhibition by PRAS40. Nature 552**:** 368-373.

838 Yuan, M., E. Pino, L. Wu, M. Kacergis and A. A. Soukas, 2012 Identification of Akt-
839 independent regulation of hepatic lipogenesis by mammalian target of rapamycin
840 (mTOR) complex 2. J Biol Chem 287**:** 29579-29588.

841 Zhang, H., J. P. Stallock, J. C. Ng, C. Reinhard and T. P. Neufeld, 2000 Regulation of
842 cellular growth by the Drosophila target of rapamycin dTOR. Genes Dev 14**:** 2712-
843 2724.

844

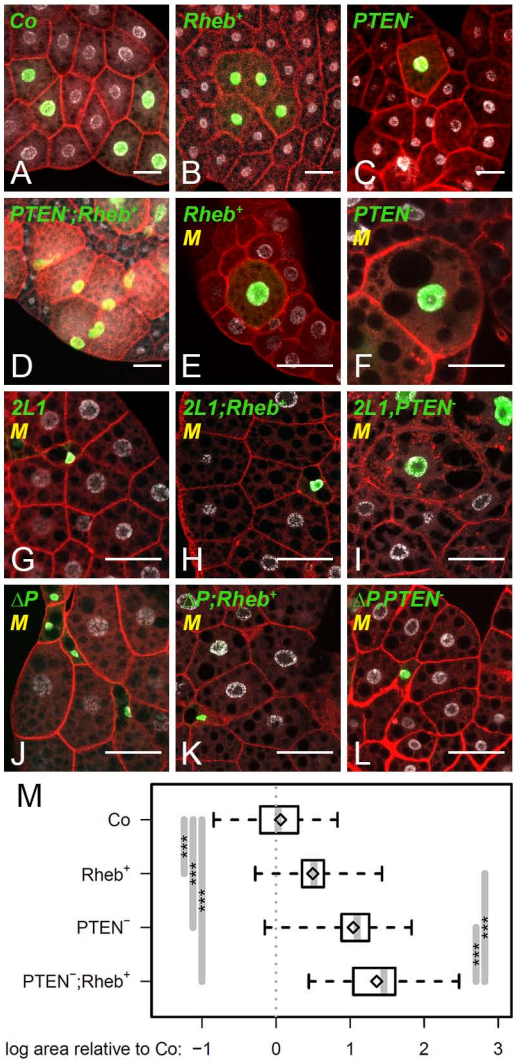
Co
Rheb+
PTEN-
A
B
C
PTEN-;Rheb+
Rheb+ M
PTEN- M
D
E
F
2L1 M
2L1;Rheb- M
2L1,PTEN- M
G
H
I
ΔP M
ΔP;Rheb+ M
ΔP,PTEN- M
J
K
L
M
Co
Rheb+
PTEN−
PTEN−;Rheb+
***
***
***
***
***
log area relative to Co: −1 0 1 2 3

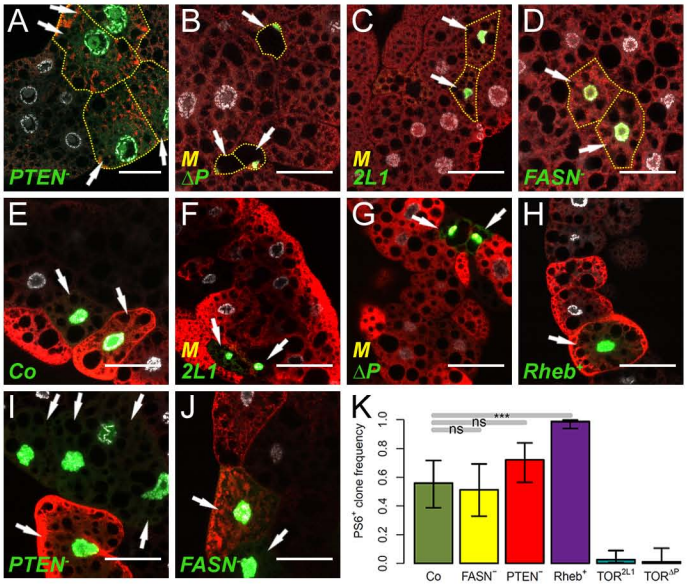
A
PTEN-
B
M
ΔP
C
M
2L1
D
FASN-
E
Co
F
M
2L1
G
M
ΔP
H
Rheb+
I
PTEN-
J
FASN-
K
PS6+ clone frequency
0.0
0.2
0.4
0.6
0.8
1.0
ns
ns
***
Co
FASN-
PTEN-
Rheb+
TOR2L1
TORΔP

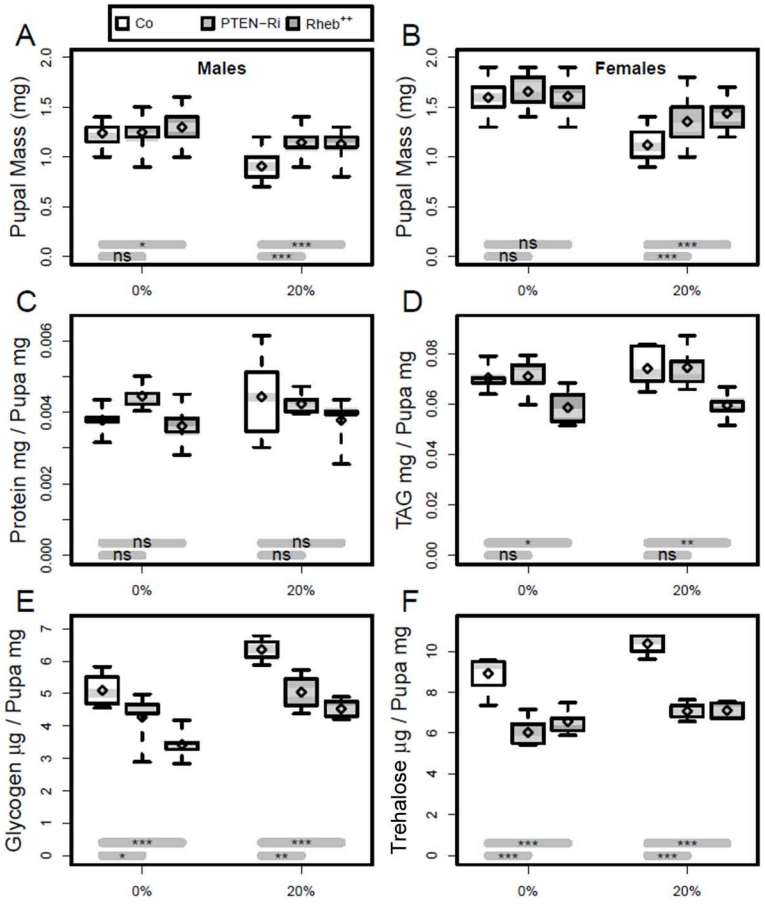
Co
PTEN−Ri
Rheb++
A
Males
Pupal Mass (mg)
B
Females
Pupal Mass (mg)
C
Protein mg / Pupa mg
D
TAG mg / Pupa mg
E
Glycogen µg / Pupa mg
F
Trehalose µg / Pupa mg
0%
20%
ns
*
**
***

A

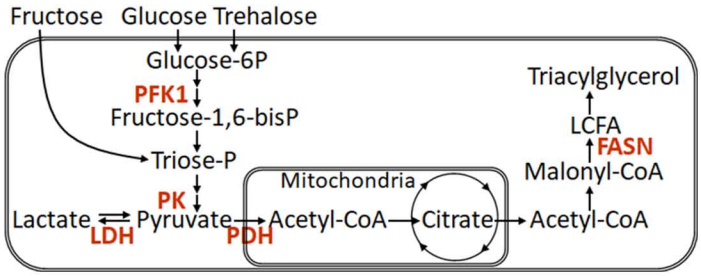

B

19°C>>29°C	0h	24h
PFK1-Ri	† L1/L2	† late L2
PK-Ri	† L2/L3	† L3/pp
LDH-Ri	† L2/L3	† L3/pp
PDH-Ri	½† L3/pp	½† L3/pp

C

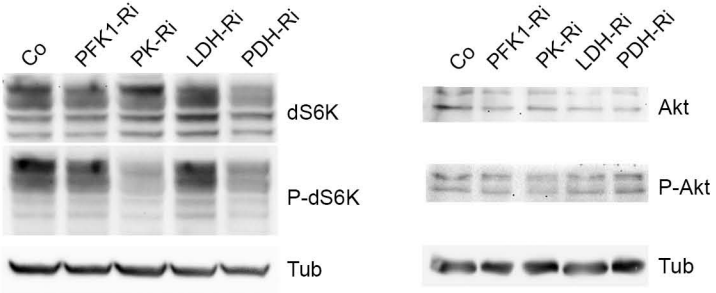

D

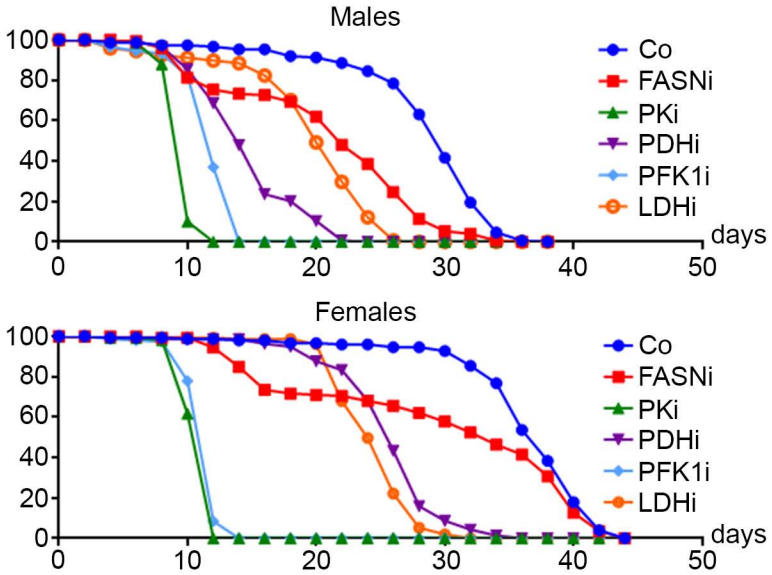

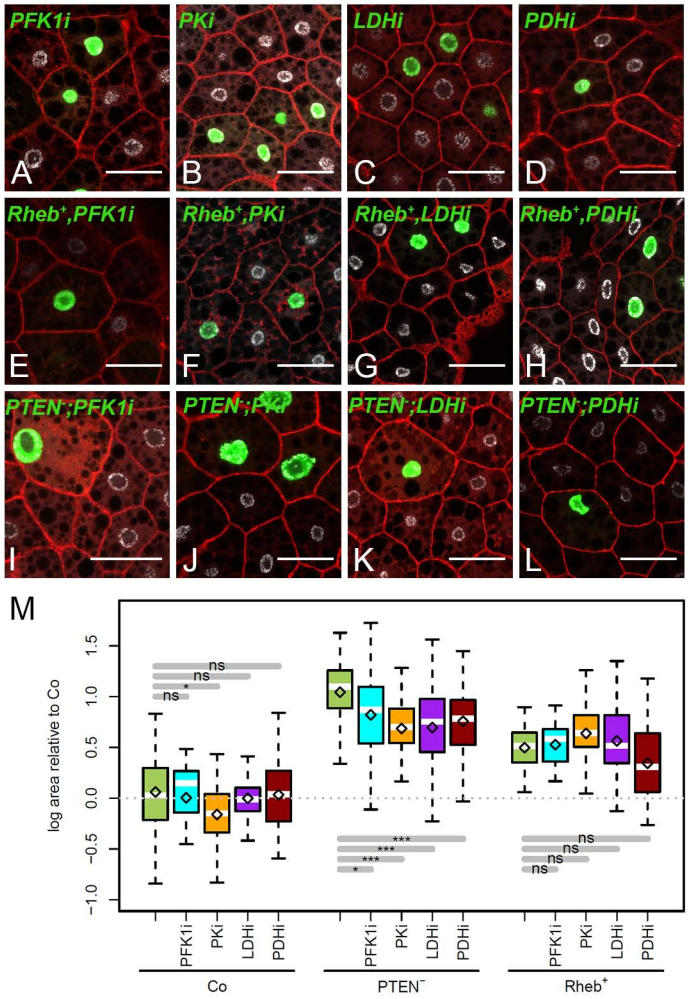
PFK1i
PKi
LDHi
PDHi
A
B
C
D
Rheb+,PFK1i
Rheb+,PKi
Rheb+,LDHi
Rheb+,PDHi
E
F
G
H
PTEN-;PFK1i
PTEN-;PKi
PTEN-;LDHi
PTEN-;PDHi
I
J
K
L
M
log area relative to Co
1.5
1.0
0.5
0.0
−0.5
−1.0
ns
ns
*
ns
***
***
***
*
ns
ns
ns
ns
PFK1i
PKi
LDHi
PDHi
Co
PTEN−
Rheb+

A

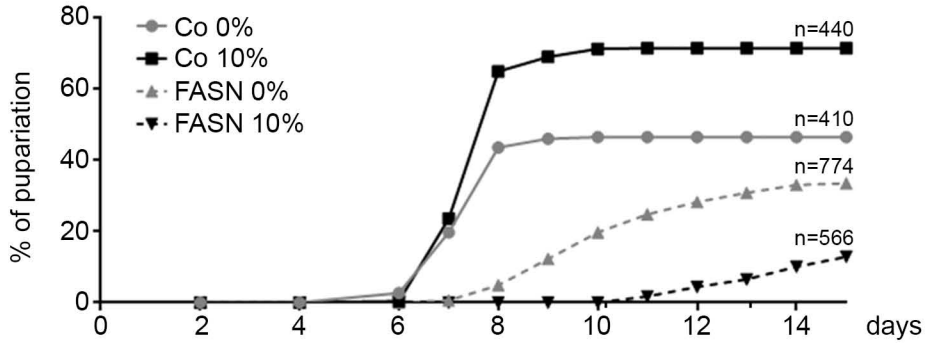
Co 0%
Co 10%
FASN 0%
FASN 10%
% of pupariation
80
60
40
20
0
0
2
4
6
8
10
12
14
days
n=440
n=410
n=774
n=566

B

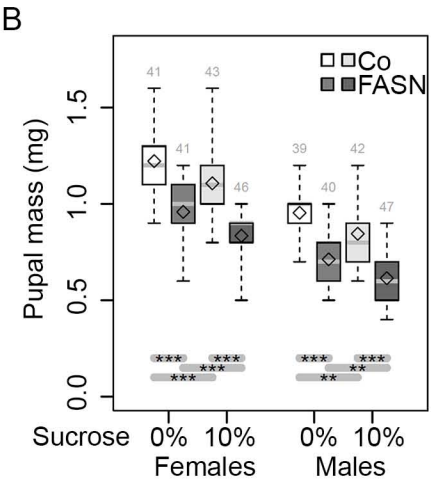
Co
FASN
Pupal mass (mg)
0.0
0.5
1.0
1.5
41
43
41
46
39
42
40
47
***
***
***
***
***
**
**
Sucrose
0%
10%
0%
10%
Females
Males

C

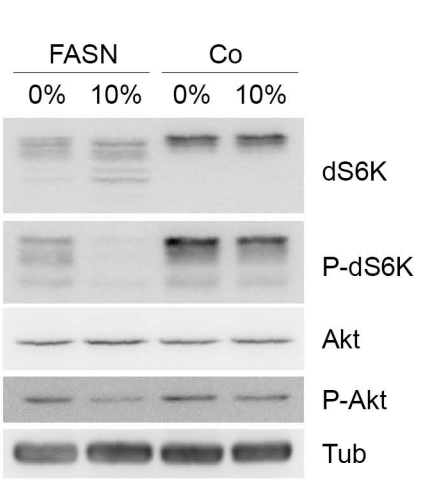
FASN
Co
0%
10%
0%
10%
dS6K
P-dS6K
Akt
P-Akt
Tub

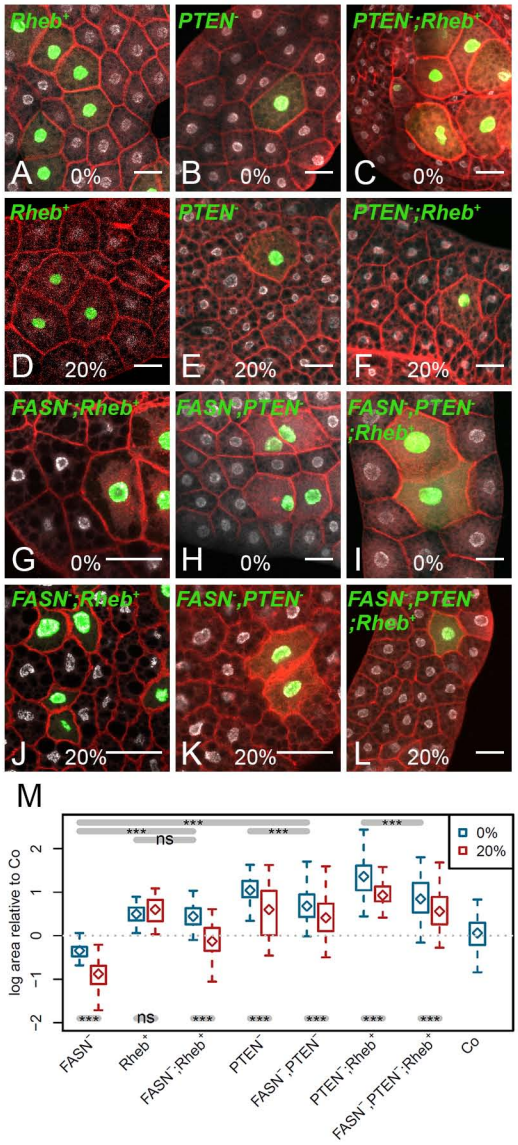
Rheb+
PTEN-
PTEN-;Rheb+
A 0%
B 0%
C 0%
Rheb+
PTEN-
PTEN-;Rheb+
D 20%
E 20%
F 20%
FASN-;Rheb+
FASN-;PTEN-
FASN-;PTEN-;Rheb+
G 0%
H 0%
I 0%
FASN-;Rheb+
FASN-;PTEN-
FASN-;PTEN-;Rheb+
J 20%
K 20%
L 20%
M
log area relative to Co
0%
20%
ns
***
FASN-
Rheb+
FASN-;Rheb+
PTEN-
FASN-;PTEN-
PTEN-;Rheb+
FASN-;PTEN-;Rheb+
Co